Association of Transmitters in Multipath Assisted Positioning

Markus Ulmschneider, Christian Gentner, Thomas Jost and Armin Dammann
German Aerospace Center (DLR), Institute of Communications and Navigation
Muenchner Str. 20, 82334 Wessling, Germany
{markus.ulmschneider,christian.gentner,thomas.jost,armin.dammann}@dlr.de

***Abstract*—A large variety of services require a precise localization. While global navigation satellite systems may show accurate positioning results in good view-to-sky conditions, their performance decreases drastically in case of shadowing and multipath propagation, such as indoors or in urban scenarios. Our approach is therefore to use terrestrial signals of opportunity for positioning. We exploit multipath propagation in a multipath assisted positioning approach: each multipath component is regarded as being emitted by a virtual transmitter in a line-of-sight condition. Since the locations of the virtual transmitters are unknown, they are estimated in addition to the user position. This results in a simultaneous localization and mapping (SLAM) problem, where physical and virtual transmitters are considered as landmarks. This paper discusses our approach named Channel-SLAM, and extends it by a solution to the data association problem. We present and compare two different methods to decide for associations among virtual transmitters. By means of simulations, we show that data association can increase the positioning performance of Channel-SLAM remarkably.**

***Index Terms*—Channel-SLAM, data association, multipath assisted positioning, simultaneous localization and mapping**

I. Introduction

The variety of applications that are based on the knowledge of the user position has led to a considerable growth in research on precise localization over the recent years. Intelligent transportation systems (ITSs) are an important field where location based services have received a lot of attention. In particular, the vision of fully autonomous vehicles has triggered research efforts. Precise positioning of vehicles in both a relative and an absolute sense is a key requirement for an autonomous vehicle. For navigation applications, the use of global navigation satellite systems (GNSSs) as a standalone system is the standard method nowadays. While the positioning performance of GNSSs tends to be good in open areas with a good view to sky, it may drastically decrease in urban areas due to signal blocking and multipath propagation. In urban canyons, tunnels or indoors, chances are that no position estimate can be obtained at all.

Especially in urban areas, for example mobile radio communication systems provide a very good coverage. Therefore, our approach uses available ground-based radio frequency (RF) signals of opportunity (SoOs) for positioning. However, multipath propagation might decrease the positioning performance drastically depending on the environment by distorting range estimates. Standard methods such as the delay locked loop try to mitigate the influence of multipath components (MPCs) on the line-of-sight (LoS) path [1].

Instead of combating multipath propagation, the idea of multipath assisted positioning is to exploit it: each MPC that arrives at a receiver can be treated as a signal sent by a virtual transmitter under a pure LoS condition. Using virtual transmitters for positioning, the minimum number of physical transmitters that is needed to locate a receiver may decrease depending on the environment. In scenarios with a lot of multipath propagation, we may be able to locate and track a receiver with a single physical transmitter.

Multipath assisted positioning schemes have been used in different ways. One idea is to use multipath propagation in a fingerprinting scheme [2]. The authors of [3], [4], for example, assume the environment to be given as a-priori knowledge in form of a floor plan, from which the virtual transmitter positions can be calculated. A similar approach has been presented in [5] for radar applications. In [6], bounds on the positioning performance are derived for this case.

In our approach named Channel-SLAM [7], [8], we do not assume any prior knowledge of the environment. Hence, the locations and delay offsets of the virtual transmitters are unknown, and we estimate them simultaneously with the user position. This approach has the structure of a simultaneous localization and mapping (SLAM) [9] problem, in which we simultaneously locate a receiver and map the physical and virtual transmitters as landmarks.

In general, using a SLAM scheme, the uncertainty about the user and landmark states increases with time. When a new landmark is observed, it is initialized with a large uncertainty about its state depending on the available measurements. Therefore, it is beneficial to know if a new landmark had been observed before, and if so, to which of the previously observed landmarks the new one corresponds. This problem is often referred to as the association problem in SLAM [10]. For example, in visual SLAM, the distinction between landmarks is based on visual features, such as shape, size or color. In our case however, the landmarks are physical or virtual transmitters, and correspond to the LoS path or MPCs, respectively. Therefore, the landmarks arise only due to reflections or scattering of the transmit signal. Since all signals components that are received via the different propagation paths contain the same data and have the same carrier frequency, finding correspondences among landmarks is a challenge that we

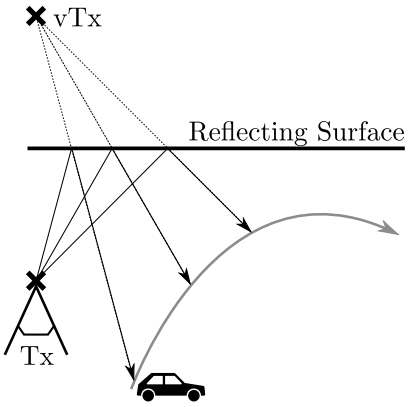

Fig. 1. Signals from the physical transmitter Tx are reflected at the straight surface and can be treated as being transmitted by the virtual transmitter vTx in a pure LoS condition. The position of vTx is the position of Tx mirrored at the surface.

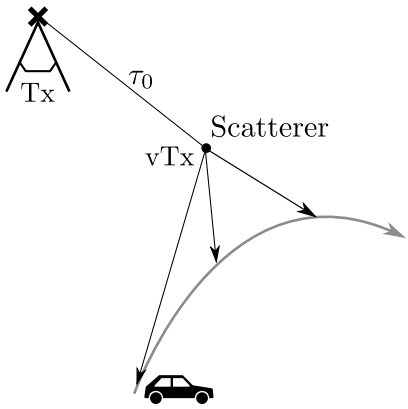

Fig. 2. Signals from the physical transmitter Tx are scattered at the punctual scatterer and can be treated as being transmitted by the virtual transmitter vTx in a pure LoS condition. The position of vTx is the position of the punctual scatterer. There is a delay offset τ_0 between the physical and virtual transmitter.

address within this paper. A first approach to reuse transmitters in Channel-SLAM based on additional, discretized user maps has been presented in [11]. In this paper, we propose a new, more general method for data association in Channel-SLAM based on [10].

The paper is organized as follows. Section II explains the idea of multipath assisted positioning and derives the current Channel-SLAM algorithm. In Section III, we extend Channel-SLAM by our solution to the association problem. An evaluation based on simulations in an urban scenario is presented in Section IV. We conclude the paper in Section V.

II. Multipath Assisted Positioning

A. Virtual Transmitters

The idea of virtual transmitters is visualized in Fig. 1. The signal emitted by the physical transmitter is reflected at the surface and arrives at the receiver as a MPC. However, the MPC can be treated as a signal originating from the virtual transmitter vTx in a pure LoS condition to the receiver. While the user moves along the trajectory, the reflection point on the wall moves as well, but the position of the virtual transmitter is static. The virtual transmitter is located at the position of the physical transmitter mirrored at the reflecting surface, and the two transmitters are inherently time synchronized.

A similar idea can be applied to the case where the signal is scattered or diffracted at a punctual scatterer as illustrated in Fig. 2. Our model of scattering is that the energy of the signal impinging on the scatterer is uniformly distributed in all directions. Then, the position of the virtual transmitter is at the scatterer itself, and the physical and the virtual transmitter are not time synchronized any more: an additional delay offset τ_0 between the two transmitters corresponding to the actual propagation distance of the signal from the physical to the virtual transmitter has to be considered. This delay offset can be interpreted as a clock offset.

The model of reflections at straight walls and scattering at punctual scatterers can be generalized to multiple reflections or scattering points [7]. If the signal is only reflected at straight walls as in Fig. 1, the delay offset τ_0 equals zero, i.e., the two transmitters are perfectly time synchronized. Otherwise, if at least one scatterer is involved, the delay offset is greater than zero.

We consider static scenarios only, where the locations of the physical transmitters and environmental objects do not change over time.

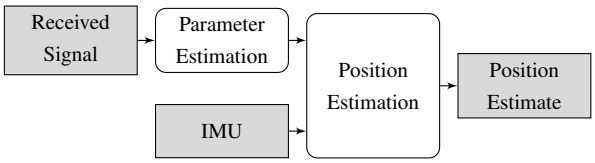

Fig. 3. Based on the received signal, the parameters of the signal components are estimated in the first step by the KEST algorithm. In the second step, the estimates serve as measurements for estimating the positions of the user and the physical and virtual transmitters. In addition, user heading rates of change measurements from an IMU are incorporated in the second step.

B. Channel-SLAM

Our approach to track the user in a two-dimensional setting consists of two steps as depicted in Fig. 3. In the first step, we estimate parameters of the signal components and track them over time using the Kalman enhanced super resolution tracking (KEST) algorithm [12]. In the second step, we fuse the KEST estimates with inertial measurement unit (IMU) data to obtain an estimate for the position of the user and the physical and virtual transmitters. Since the first step is connected to estimating the channel impulse response (CIR), and the second part essentially solves a SLAM problem, we named our approach Channel-SLAM [7]. The Channel-SLAM algorithm does not differentiate between physical and virtual transmitters. In the following, the term transmitter is therefore a general term for physical and virtual transmitters.

We assume the wireless multipath channel to be linear and time-variant. Hence, we express the CIR $h(\tau, t)$ at time t and delay τ as a sum of signal components with complex

amplitudes $\alpha_i(t)$ and times of arrival (ToAs) $d_i(t)$ [13],

$$h(\tau, t) = \sum_i \alpha_i(t)\delta(\tau - d_i(t)). \quad (1)$$

We use the KEST algorithm presented in [12] to detect and track the complex amplitudes, the ToAs and the angles of arrival (AoAs) in the azimuth plane, $\theta_i(t)$, for each signal component i. The KEST algorithm is composed of two stages. The inner stage applies a maximum likelihood (ML) estimator to estimate the parameters of each signal component. In an outer stage, these parameters are tracked over time by a Kalman filter. In addition, the overall number of signal components is tracked.

We estimate the complex amplitudes only for a better signal component tracking performance, and do not use them further during the position estimation. Hence, after sampling from the received signal, the measurement vector at time step k is

$$\boldsymbol{z}_k = \begin{bmatrix} \boldsymbol{d}_k^T & \boldsymbol{\theta}_k^T \end{bmatrix}^T, \quad (2)$$

where

$$\boldsymbol{d}_k = [d_{1,k} \ \dots \ d_{N_{\text{TX}},k}]^T, \quad (3)$$

are the ToA estimates and

$$\boldsymbol{\theta}_k = [\theta_{1,k} \ \dots \ \theta_{N_{\text{TX}},k}]^T, \quad (4)$$

are the AoA estimates from KEST at time step k. The number of propagation paths, or signal components, is denoted by N_{TX}. Note that N_{TX} corresponds to the number of transmitters, and may change over time. However, for notational convenience, we drop the time step index k in N_{TX}.

The state vector $\boldsymbol{x}_k$ that is to be estimated at each time step k consists of the user state $\boldsymbol{x}_{\text{u},k}$ and the transmitters' state $\boldsymbol{x}_{\text{TX},k}$, i.e.,

$$\begin{aligned} \boldsymbol{x}_k &= \begin{bmatrix} \boldsymbol{x}_{\text{u},k}{}^T & \boldsymbol{x}_{\text{TX},k}{}^T \end{bmatrix}^T \\ &= \begin{bmatrix} \boldsymbol{x}_{\text{u},k}{}^T & \boldsymbol{x}_{\text{TX},k}^{<1>T} & \dots & \boldsymbol{x}_{\text{TX},k}^{<N_{\text{TX}}>T} \end{bmatrix}^T, \end{aligned} \quad (5)$$

where $\boldsymbol{x}_{\text{TX},k}^{<j>}$ is the state of the j^{th} transmitter. The user state consists of the position and velocity in two dimensions, which is

$$\boldsymbol{x}_{\text{u},k} = [x_k \ \ y_k \ \ v_{x,k} \ \ v_{y,k}]^T. \quad (6)$$

The state of the j^{th} transmitter includes its location and its clock offset τ_0 to the receiver, namely

$$\boldsymbol{x}_{\text{TX},k}^{<j>} = \begin{bmatrix} x_{\text{TX},k}^{<j>} & y_{\text{TX},k}^{<j>} & \tau_{0,k}^{<j>} \end{bmatrix}^T. \quad (7)$$

Our goal is to estimate the state vector for all time steps, i.e., $\boldsymbol{x}_{0:k}$, based on the measurements $\boldsymbol{z}_{1:k}$. Therefore, we calculate the posterior distribution of the user and transmitter states recursively over time in a Bayesian recursive estimation context [14]. Using Rao-Blackwellization, we can factorize this posterior distribution conditioned on the measurements $\boldsymbol{z}_{1:k}$ as

$$\begin{aligned} \mathrm{p}\left(\boldsymbol{x}_{0:k}|\boldsymbol{z}_{1:k}\right) &= \mathrm{p}\left(\boldsymbol{x}_{\text{TX},0:k}, \boldsymbol{x}_{\text{u},0:k}|\boldsymbol{z}_{1:k}\right) \\ &= \mathrm{p}\left(\boldsymbol{x}_{\text{u},0:k}|\boldsymbol{z}_{1:k}\right) \times \mathrm{p}\left(\boldsymbol{x}_{\text{TX},0:k}|\boldsymbol{z}_{1:k}, \boldsymbol{x}_{\text{u},0:k}\right). \end{aligned} \quad (8)$$

The first factor in the second line of Eq. (8) is the posterior distribution of the user state $\boldsymbol{x}_{\text{u},0:k}$ for time step 0 to k. The second factor in the same line denotes the posterior distribution of the transmitters state $\boldsymbol{x}_{\text{TX},0:k}$ for time step 0 to k conditioned on the user state. The measurements $\boldsymbol{z}_{1:k}$ are obtained from Eq. (2). We assume independence among the measurements for each transmitter, and factorize the conditioned posterior distribution of $\boldsymbol{x}_{\text{TX},0:k}$ as

$$\mathrm{p}\left(\boldsymbol{x}_{\text{TX},0:k}|\boldsymbol{z}_{1:k}, \boldsymbol{x}_{\text{u},0:k}\right) = \prod_{j=1}^{N_{\text{TX}}} \mathrm{p}\left(\boldsymbol{x}_{\text{TX},0:k}^{<j>}|\boldsymbol{z}_{1:k}^{<j>}, \boldsymbol{x}_{\text{u},0:k}\right). \quad (9)$$

The assumption of independence among transmitter measurements allows to estimate the state vector of each transmitter independently.

Bayesian recursive estimation schemes work in two recursively executed steps, namely the prediction and the update step [14]. In the prediction step of the user, we make use of heading rate of change measurements from a gyroscope in an IMU. For a detailed explanation of the implementation, we refer the reader to [7], [8]. However, note that we do incorporate only heading rate of change measurements from a gyroscope, but no acceleration measurements. The speed of the user is modeled by a random walk model.

Since we consider a static environment, the transmitter positions and clock offsets are constant. Hence, in the prediction step of the transmitters' state vector, the transition prior of the j^{th} transmitter can be expressed as

$$\mathrm{p}\left(\boldsymbol{x}_{\text{TX},k}^{<j>}|\boldsymbol{x}_{\text{TX},k-1}^{<j>}\right) = \delta\left(\boldsymbol{x}_{\text{TX},k}^{<j>} - \boldsymbol{x}_{\text{TX},k-1}^{<j>}\right), \quad (10)$$

where $\delta(\cdot)$ denotes the Dirac distribution.

In the update steps of both the user and the transmitters, the measurement noise samples for the ToA and AoA measurements are assumed to be drawn from uncorrelated zero-mean Gaussian distributions with variances $\sigma_{d,j}^2$ and $\sigma_{\theta,j}^2$, respectively, for the j^{th} transmitter. The likelihood $\mathrm{p}\left(\boldsymbol{z}_k|\boldsymbol{x}_k\right)$ for the measurement vector $\boldsymbol{z}_k$ conditioned on the state vector $\boldsymbol{x}_k$ can then be expressed as the product

$$\mathrm{p}\left(\boldsymbol{z}_k|\boldsymbol{x}_k\right) = \prod_{j=1}^{N_{\text{TX}}} \mathcal{N}\Big(d_{j,k}; \hat{d}_{j,k}, \sigma_{d,j}^2\Big)\, \mathcal{N}\Big(\theta_{j,k}; \hat{\theta}_{j,k}, \sigma_{\theta,j}^2\Big), \quad (11)$$

where $\mathcal{N}\left(x; \mu, \sigma^2\right)$ denotes a Gaussian probability density function (PDF) in x with mean μ and variance σ^2. The predicted ToA between the user and the j^{th} transmitter is calculated as

$$\hat{d}_{j,k} = \frac{1}{c_0}\sqrt{(x_k - x_{\text{TX},k}^{<j>})^2 + (y_k - y_{\text{TX},k}^{<j>})^2} + \tau_{0,k}^{<j>}, \quad (12)$$

where c_0 denotes the speed of light. The corresponding predicted AoA is

$$\hat{\theta}_{j,k} = \text{atan2}\left(y_k - y_{\text{TX},k}^{<j>}, x_k - x_{\text{TX},k}^{<j>}\right) - \text{atan2}\left(v_{y,k}, v_{x,k}\right), \quad (13)$$

where the function atan2 (y, x) calculates the four quadrant inverse tangent function, returning the counter-clockwise angle between the positive x-axis and the point given by the coordinates (x, y).

For the actual estimation of the state, we use a Rao-Blackwellized particle filter as in [7]. The user state is estimated by an outer particle filter. Each of the user particles represents one hypotheses for the user state, and has N_{TX} inner particle filters that estimate the states of the N_{TX} transmitters associated to it. The posterior distribution of the user state is approximated by [15]

$$\mathrm{p}\left(\boldsymbol{x}_{\mathrm{u},k}|\boldsymbol{z}_{1:k}\right) = \sum_{i=1}^{N_p} w_k^{<i>}\delta\left(\boldsymbol{x}_{\mathrm{u},k} - \boldsymbol{x}_{\mathrm{u},k}^{<i>}\right), \tag{14}$$

where $\boldsymbol{x}_{\mathrm{u},k}^{<i>}$ is the i^{th} user particle, $w_k^{<i>}$ its associated weight, and N_p the number of user particles. Similarly, the posterior distribution of the state of the j^{th} transmitter of the i^{th} user particle is approximated as

$$\mathrm{p}\left(\boldsymbol{x}_{\mathrm{TX},k}^{<i,j>}|\boldsymbol{z}_{1:k}\right) = \sum_{l=1}^{N_{p,\mathrm{Tx}}} w_k^{<i,j,l>}\delta\left(\boldsymbol{x}_{\mathrm{TX},k}^{<i,j>} - \boldsymbol{x}_{\mathrm{TX},k}^{<i,j,l>}\right), \tag{15}$$

where $\boldsymbol{x}_{\mathrm{TX},k}^{<i,j,l>}$ is the l^{th} particle of the j^{th} transmitter of the i^{th} user particle, $w_k^{<i,j,l>}$ its associated weight, and $N_{p,\mathrm{Tx}}$ the number of transmitter particles. The update of the weight of the i^{th} user particle can be expressed by the proportionality

$$w_k^{<i>} \propto w_{k-1}^{<i>}\mathrm{p}\left(\boldsymbol{z}_k|\boldsymbol{x}_{\mathrm{u},k}^{<i>}\right). \tag{16}$$

For a detailed description of how to calculate the weights in the particle filter for the user and the transmitters, we refer to [7], [15].

The KEST algorithm tracks signal components over time as described above. Whenever the KEST algorithm detects a new signal component, a new transmitter is initialized based on the measurement $\boldsymbol{z}_k$, i.e., the ToA and AoA estimates of KEST. When the KEST algorithm loses track of a signal component, the corresponding transmitter is not observable any more. In the current version of Channel-SLAM, it does not contribute to the location estimation any further.

III. The Association Problem

In the Channel-SLAM algorithm [7], [8] summarized in Section II, every signal component, or propagation path, corresponds to one transmitter. However, the KEST algorithm may lose and regain track of signal components. Hence, two or more signal components that are received at different time steps may originate from the same transmitter. This situation is depicted in Fig. 4. The LoS signal from a transmitter is received in Region I, but blocked by an obstacle in Region II. When the signal is received again by the user in Region III, the KEST algorithm initializes a new signal component, and hence a new transmitter is assumed. This new transmitter is the same transmitter observed before in Region I, though. Similarly, the KEST algorithm may lose track of a signal component when its received signal strength is very low, or if

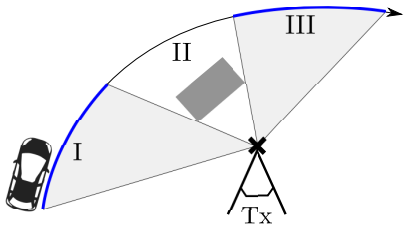

Fig. 4. As the user moves on its track, the LoS signal in Region I to the transmitter is lost in Region II temporarily due to blocking by an obstacle. In Region III, the signal is obtained again.

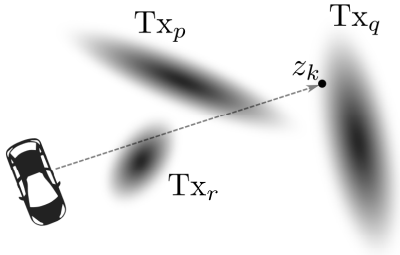

Fig. 5. Based on the new measurement $\boldsymbol{z}_k$ at the receiver, a new transmitter may be initialized, or the measurement may be associated with any of the three previously observable transmitters Tx_p,Tx_q, or Tx_r. The ellipses represent the estimated posterior distributions of the transmitter states.

there is another signal component with similar parameters and higher signal strength. When the strength of the lost signal component increases again, the KEST algorithm might start tracking it again assuming a new transmitter.

When KEST detects a new signal component, a new transmitter is initialized, and there are two possible cases:

1) the new transmitter is indeed a new transmitter that has never been observed before, or
2) the new transmitter corresponds to an 'old' transmitter that had been observed before.

Data association describes the question for which case to decide, and, in the second case, to which old transmitter the new one corresponds.

Fig. 5 illustrates the association problem with an example. The ellipses represent the position posterior distributions of the previously, but not currently observed transmitters Tx_p,Tx_q, and Tx_r. When the KEST algorithm detects a new signal component with a ToA and AoA measurement, the corresponding new transmitter is either initialized based on the measurement, or it may be associated with one of the old transmitters Tx_p,Tx_q, and Tx_r. In the latter case, the new transmitter is initialized using the previously estimated posterior distribution of the corresponding old transmitter. Note that due to the clock offsets of the transmitters, each of the associations with Tx_p,Tx_q, and Tx_r may be more or less likely, leading to ambiguities.

Correct associations can improve the positioning performance, as the uncertainty about the state of a new transmitter is high upon initialization. On the one hand, this is because the uncertainty about the user state tends to increase over time, and new transmitters might therefore be initialized with a

high uncertainty as well. On the other hand, the measurements cover only two dimensions, i.e., ToA and AoA, whereas the transmitter state vectors are of three dimensions as in Eq. (7). Note that also for the data association, we do not take into account the amplitudes of the signal components estimated by KEST, since the assumption of perfectly scattering and reflecting objects does not hold in practice due to the shape or materials of these objects. Hence, a measurement covers only a subspace of the transmitters' state vector, leading to an underdetermined problem for each single time step. Only when the user moves through the scenario and takes measurements from a sufficient number of different points in space, the posterior distribution of a transmitter can converge. If prior information in terms of a correct association can be used for initialization of a transmitter, the uncertainty about that transmitter tends to be smaller upon initialization, and the user state estimate can be corrected up to a certain extent.

However, wrong associations can make the filter diverge. Since we face an underdetermined problem in each time step as described above, association ambiguities might arise. It is of high importance to prevent wrong associations in the first place, or to resolve them during the filtering process. Therefore, we use a multiple hypothesis tracking (MHT) method for the associations among transmitters. As we use a particle filter to track the posterior distribution of the user state, the user state is represented by a number of particles with associated weights. A MHT method is very suitable to this kind of filter, since association decisions can be made based on each particle individually. Hence, each particle carries a hypothesis on the associations among transmitters.

When a new signal component is detected at time step k by the KEST algorithm, a new transmitter is initialized. The variable n_k describes the association of the new transmitter to the previously observable transmitter n_k. A set of association decisions made by particle i up to time step k is denoted by $\hat{n}_k^{<i>}$. Within the scope of this paper, we assume that KEST initializes no more than one signal component at each time step.

The marginalized likelihood of the measurement at time step k for particle i assuming that a newly detected signal component with measurements contained in $\boldsymbol{z}_k$ corresponds to the old transmitter n_k is denoted by [10]

$$p_{n_k} = \mathrm{p}\left(\boldsymbol{z}_k | n_k, \hat{n}_{k-1}^{<i>}, \boldsymbol{x}_{\mathrm{u},k}^{<i>}, \boldsymbol{z}_{1:k-1}\right). \tag{17}$$

We can calculate p_{n_k} as

$$\begin{aligned}&\mathrm{p}\left(\boldsymbol{z}_k | n_k, \hat{n}_{k-1}^{<i>}, \boldsymbol{x}_{\mathrm{u},k}^{<i>}, \boldsymbol{z}_{1:k-1}\right)\\ &= \int \mathrm{p}\left(\boldsymbol{z}_k | \boldsymbol{x}_{\mathrm{TX},k}^{<i,n_k>}, n_k, \hat{n}_{k-1}^{<i>}, \boldsymbol{x}_{\mathrm{u},k}^{<i>}, \boldsymbol{z}_{1:k-1}\right)\\ &\quad \times \mathrm{p}\left(\boldsymbol{x}_{\mathrm{TX},k}^{<i,n_k>} | n_k, \hat{n}_{k-1}^{<i>}, \boldsymbol{x}_{\mathrm{u},k}^{<i>}, \boldsymbol{z}_{1:k-1}\right) \mathrm{d}\boldsymbol{x}_{\mathrm{TX},k}^{<i,n_k>},\end{aligned} \tag{18}$$

where $\boldsymbol{x}_{\mathrm{TX},k}^{<i,n_k>}$ denotes the state vector of the $n_k{}^{\text{th}}$ transmitter for the i^{th} user particle.

Assuming a hidden Markov model, the first integrand in Eq. (18) can be simplified to

$$\begin{aligned}&\mathrm{p}\left(\boldsymbol{z}_k | \boldsymbol{x}_{\mathrm{TX},k}^{<i,n_k>}, n_k, \hat{n}_{k-1}^{<i>}, \boldsymbol{x}_{\mathrm{u},k}^{<i>}, \boldsymbol{z}_{1:k-1}\right)\\ &= \mathrm{p}\left(\boldsymbol{z}_k | \boldsymbol{x}_{\mathrm{TX},k}^{<i,n_k>}, n_k, \hat{n}_{k-1}^{<i>}, \boldsymbol{x}_{\mathrm{u},k}^{<i>}\right).\end{aligned} \tag{19}$$

Since we use a particle filter to estimate transmitter states, the transmitter posterior distributions are represented by particles with associated weights. The second integrand in Eq. (18) can therefore be rewritten similarly to Eq. (15) as

$$\begin{aligned}&\mathrm{p}\left(\boldsymbol{x}_{\mathrm{TX},k}^{<i,n_k>} | n_k, \hat{n}_{k-1}^{<i>}, \boldsymbol{x}_{\mathrm{u},k}^{<i>}, \boldsymbol{z}_{1:k-1}\right)\\ &= \sum_{l=1}^{N_{p,\mathrm{Tx}}} w_k^{<i,n_k,l>} \delta\left(\boldsymbol{x}_{\mathrm{TX},k}^{<i,n_k>} - \boldsymbol{x}_{\mathrm{TX},k}^{<i,n_k,l>}\right),\end{aligned} \tag{20}$$

where $\boldsymbol{x}_{\mathrm{TX},k}^{<i,j,l>}$ is the l^{th} particle of the j^{th} transmitter of the i^{th} user particle, and $w_k^{<i,j,l>}$ its associated weight. Thus, we have for p_{n_k} in Eq. (17)

$$\begin{aligned}p_{n_k} &= \mathrm{p}\left(\boldsymbol{z}_k | n_k, \hat{n}_{k-1}^{<i>}, \boldsymbol{x}_{\mathrm{u},k}^{<i>}, \boldsymbol{z}_{1:k-1}\right)\\ &= \sum_{l=1}^{N_{p,\mathrm{Tx}}} w_k^{<i,n_k,l>} \mathrm{p}\left(\boldsymbol{z}_k | \boldsymbol{x}_{\mathrm{TX},k}^{<i,n_k,l>}, n_k, \hat{n}_{k-1}^{<i>}, \boldsymbol{x}_{\mathrm{u},k}^{<i>}\right).\end{aligned} \tag{21}$$

At each time step k, we have a set Υ_k of previously tracked transmitters that are currently not observable any more. When KEST loses track of a signal component, the corresponding transmitter is added to Υ_k. When a new transmitter is to be initialized, the marginalized likelihoods p_{n_k} for the measurement $\boldsymbol{z}_k$ are calculated as in Eq. (21) for each old transmitter $n_k \in \Upsilon_k$.

In order to reduce the computational complexity, we regard only those old transmitters for associations for which p_{n_k} exceeds a threshold ρ. We denote a set of indices of these transmitters by Γ_k. Thus, we have

$$\Gamma_k = \{j : j \in \Upsilon_k \wedge p_j > \rho\}. \tag{22}$$

Association decisions are made based on each particle i individually, and there are different ways to come to a decision. For the ML method, the association for which p_{n_k} from Eq. (21) is the highest is chosen, if at least one probability p_j of a transmitter $j \in \Gamma_k$ is greater than a threshold p_0. In this case we have

$$\hat{n}_{\mathrm{ML},k}^{<i>} = \underset{n_k \in \Gamma_k}{\arg\max}\ p_{n_k}, \tag{23}$$

and the new transmitter is associated to transmitter $\hat{n}_{\mathrm{ML},k}^{<i>}$, i.e., it is initialized with the estimated posterior distribution of transmitter $\hat{n}_{\mathrm{ML},k}^{<i>}$. If no p_j exceeds p_0, no association is made, and the new transmitter is initialized without any prior information, but with the first ToA and AoA estimate from KEST for the corresponding signal component.

An alternative to the ML method is data association sampling (DAS). In DAS, we sample associations randomly from the probabilities $c\,p_{n_k}$ for $n_k \in \Gamma_k$ and the probability $c\,p_0$ representing no association. The variable c is a normalizing

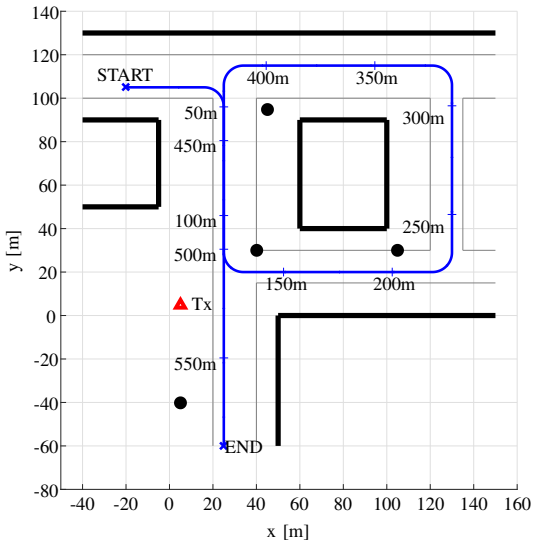

Fig. 6. The urban simulation scenario. There is one physical transmitter Tx. The user travels along the blue track from START to END. The user traveled distance is marked at every $50\,\mathrm{m}$. The black lines represent walls that reflect RF signals, black dots represent punctual scatterers.

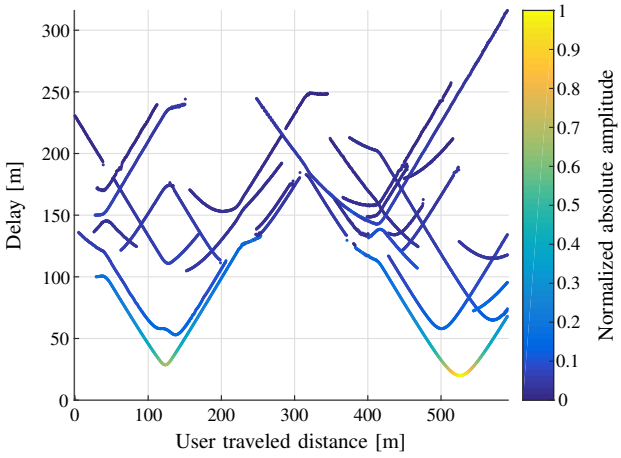

Fig. 7. Results of the KEST algorithm, where signal components with a long life span are extracted. The delays of the signal components, which are the estimated ToAs multiplied by the speed of light, are plotted versus the user traveled distance. Hence, each line describes the evolution of a signal component. The absolute values of the normalized amplitudes of the signal components are indicated by the colors.

constant. While the association resulting in the highest p_{n_k} is chosen deterministically in the the ML approach, the randomness in DAS allows less likely association decisions. On the one hand, this tends to increase the number of particles required and therefore the computational complexity. On the other hand, DAS is more robust. In particular, in case of measurement ambiguities, we expect the DAS scheme to outperform the ML method.

IV. Simulations

We performed simulations to evaluate our data association approach. A top view of the urban multipath scenario is depicted in Fig. 6. The thick black lines represent walls that reflect the RF transmit signal, and the black dots model punctual scatterers such as traffic light poles. In the scenario, there is one physical transmitter marked by the red triangle labeled Tx. The blue line represents the track of a car equipped with a receiver traveling from START to END with one loop around the central building. The traveled distance of the user is marked at every $50\,\mathrm{m}$. The car moves with a constant velocity of $10\,\mathrm{m/s}$. Each $0.05\,\mathrm{ms}$, the receiver records a snapshot of the received signal.

With a ray tracing approach, we simulate the CIR and the received signal for each snapshot as input for the KEST algorithm. The physical transmitter continuously emits a signal of rectangular shape in frequency domain with a bandwidth of $100\,\mathrm{MHz}$ and a center frequency of $1.51\,\mathrm{GHz}$. For simplicity, we assume an additive white Gaussian noise (AWGN) channel with free-space path loss. Each reflection of the RF signal causes a power loss of $3\,\mathrm{dB}$, and each scattering a power loss of $6\,\mathrm{dB}$. The signal-to-noise-ratio (SNR) at the receiver averaged over the entire receiver track is $8.74\,\mathrm{dB}$. The receiver is equipped with a two-dimensional antenna array consisting of nine elements to obtain ToA and AoA estimates of the impinging signal components.

Since Channel-SLAM considers an underdetermined system, we prefer signal components that are visible over a long time span. Hence, we choose only those signal components from the KEST algorithm that have a long life span. For our simulations, we use all signal components that are observable for a user traveled distance of at least $38\,\mathrm{m}$ as shown in Fig. 7. The delay and amplitude of the signal components are plotted versus the user traveled distance. Note that the AoAs of the components are not shown here, and the delays are the ToA estimates multiplied by the speed of light and hence in meter. The absolute values of the amplitudes are normalized in linear domain.

The user travels through the urban scenario on the trajectory as described above. We assume only the starting position and direction of the user to be known roughly to create a local coordinate system. The user particles are initially distributed normally around the true user position with a variance of $1\,\mathrm{m}^2$. The average root mean square error (RMSE) over 150 runs of the user versus the user traveled distance is plotted in Fig. 8 for different cases. The red curve describes the RMSE if no associations are made among transmitters. In this case, each time a new signal component is detected by the KEST algorithm, a new transmitter is initialized with the available ToA and AoA estimates from the KEST algorithm. The blue curve shows the RMSE for the ML method, and the green curve for DAS.

Since we assume the initial state of the user to be known, the RMSE is small in the beginning and increases after the first meters for all curves as expected. For the red curve, where no associations are made, the RMSE stays constant after a traveled distance of approx. $230\,\mathrm{m}$ and even decreases when the

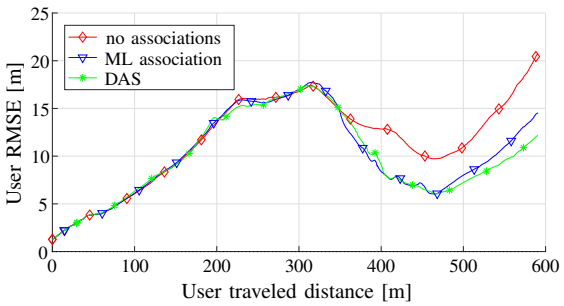

Fig. 8. The RMSE of the user position versus the user traveled distance. The RMSE is plotted in the case that no associations among transmitters are made in red, for the ML association method in blue and for DAS in green.

user gets back in a LoS condition to the physical transmitter. Towards the end of the track, the RMSE increases again with a final value of $20.8\,\mathrm{m}$. The reason for the increasing RMSE might be the high geometrical delusion of precision (GDOP) value at the end of the track, where all signal components arrive at the user from a similar direction.

For the ML association and the DAS method, represented by the blue respectively green curve, the positioning performance is very similar during the first $470\,\mathrm{m}$ of traveled distance. After approx. $370\,\mathrm{m}$, both association methods show a performance gain. At this part of the track, several transmitters that had been observed in the beginning are observed again, and are reused by associations. Hence, the RMSE drops significantly for both the ML and the DAS method. However, both suffer from the high GDOP value at the end of the track, where the RMSE increases again. Towards the end of the track, DAS shows a slightly better positioning performance than the ML method. We assume that this is due to the relatively large number of transmitters that are observable in this area, and hence possible ambiguities in associations. The ML method chooses the most likely associations, which might be wrong though, while the DAS method samples associations making the scheme more robust. The final RMSE values are $14.6\,\mathrm{m}$ for the ML method and $12.5\,\mathrm{m}$ for DAS.

An interesting observation are the small scale fluctuations in the RMSE for both association methods. They occur when a number of particles decide for wrong associations, causing the RMSE to increase. When the measurement probabilities for these particles in future time steps become small, the particles are unlikely to be resampled, and the RMSE decreases again. Such an effect can be observed after a traveled distance of approx. $390\,\mathrm{m}$, for example.

V. Conclusion

Within this paper, we extended the Channel-SLAM algorithm by a solution to the association problem. In multipath assisted positioning, a transmitter that had been observable before might be observed again at a later point, and an association can be made. We presented and compared two different ways to decide for associations among transmitters on a particle basis, a ML and a DAS method. Both methods are MHT schemes. Our simulations showed that the positioning error for a user decreases remarkably when data association schemes are used in Channel-SLAM, and DAS performs slightly better than the ML method.

VI. Acknowledgement

This work was partially supported by the EU project HIGHTS (High precision positioning for cooperative ITS applications) MG-3.5a-2014-636537 and the DLR project Dependable Navigation.

References

[1] M. Lentmaier and B. Krach, "Maximum Likelihood Multipath Estimation in Comparison with Conventional Delay Lock Loops," in *Proceedings of the 19th International Technical Meeting of the Satellite Division of The Institute of Navigation (ION GNSS)*, Sep. 2006.

[2] M. Triki, D. T. M. Slock, V. Rigal, and P. Francois, "Mobile Terminal Positioning via Power Delay Profile Fingerprinting: Reproducible Validation Simulations," in *IEEE Vehicular Technology Conference*, Sept 2006, pp. 1–5.

[3] P. Meissner and K. Witrisal, "Multipath-assisted single-anchor indoor localization in an office environment," in *Systems, Signals and Image Processing (IWSSIP), 2012 19th International Conference on*, Apr. 2012, pp. 22–25.

[4] E. Leitinger, P. Meissner, M. Lafer, and K. Witrisal, "Simultaneous localization and mapping using multipath channel information," in *2015 IEEE International Conference on Communication Workshop (ICCW)*, Jun. 2015, pp. 754–760.

[5] P. Setlur, G. Smith, F. Ahmad, and M. Amin, "Target Localization with a Single Sensor via Multipath Exploitation," *IEEE Trans. Aerosp. Electron. Syst.*, vol. 48, no. 3, pp. 1996–2014, Jul. 2012.

[6] P. Setlur and N. Devroye, "Multipath exploited Bayesian and Cramer-Rao bounds for single-sensor target localization," *EURASIP Journal on Advances in Signal Processing*, vol. 2013, no. 1, p. 53, 2013.

[7] C. Gentner, T. Jost, W. Wang, S. Zhang, A. Dammann, and U.-C. Fiebig, "Multipath Assisted Positioning with Simultaneous Localization and Mapping," *IEEE Trans. Wireless Commun.*, vol. 15, no. 9, pp. 6104–6117, Sep. 2016.

[8] M. Ulmschneider, C. Gentner, R. Raulefs, and M. Walter, "Multipath Assisted Positioning in Vehicular Applications," in *13th Workshop on Positioning, Navigation and Communications (WPNC)*, Oct. 2016.

[9] H. Durrant-Whyte and T. Bailey, "Simultaneous localization and mapping: part I," *IEEE Robot. Autom. Mag.*, vol. 13, no. 2, pp. 99–110, Jun. 2006.

[10] S. Thrun, M. Montemerlo, D. Koller, B. Wegbreit, J. Nieto, and E. Nebot, "FastSLAM: An Efficient Solution to the Simultaneous Localization And Mapping Problem with Unknown Data Association," *Journal of Machine Learning Research*, vol. 4, no. 3, pp. 380–407, 2004.

[11] C. Gentner, B. Ma, M. Ulmschneider, T. Jost, and A. Dammann, "Simultaneous Localization and Mapping in Multipath Environments," in *Proceedings of the IEEE/ION Position Location and Navigation Symposium (PLANS), Savannah, Georgia, USA*, Apr. 2016.

[12] T. Jost, W. Wang, U. Fiebig, and F. Perez-Fontan, "Detection and Tracking of Mobile Propagation Channel Paths," *IEEE Trans. Antennas Propag.*, vol. 60, no. 10, pp. 4875–4883, Oct. 2012.

[13] D. Tse and P. Viswanath, *Fundamentals of Wireless Communication*. Cambridge University Press, 2005.

[14] S. Kay, *Fundamentals of Statistical Signal Processing: Estimation Theory*, ser. Fundamentals of Statistical Signal Processing. Prentice-Hall PTR, 1998, no. Bd. 1.

[15] M. Arulampalam, S. Maskell, N. Gordon, and T. Clapp, "A Tutorial on Particle Filters for Online Nonlinear/non-Gaussian Bayesian Tracking," *IEEE Trans. Signal Process.*, vol. 50, no. 2, pp. 174–188, Feb. 2002.